

Two-photon, two-color polarization spectroscopy of the $3s^2S_{1/2} \rightarrow 5s^2S_{1/2}$ transition in atomic Na: Measurement of relative transition matrix elements

Rodney P. Meyer, A. I. Beger, and M. D. Havey

Physics Department, Old Dominion University, Norfolk, Virginia 23529

(Received 7 August 1996)

Precise measurements are reported on the linear polarization spectrum associated with two-photon, two-color spectroscopy of the $3s^2S_{1/2} \rightarrow 5s^2S_{1/2}$ transition in atomic Na. Measurements are made in an approximately 40-cm^{-1} range in the vicinity of the $3p^2P_j$ ($j=1/2, 3/2$) levels, which serve as the principal intermediate levels for the two-photon transitions. Because of interference between the transition amplitudes through each fine-structure multiplet component, the polarization varies from nearly 100% to -100% within this spectral range. Modeling the data to include the effects of more energetic p levels and allowing for a j -dependent ratio of transition amplitudes R results in an excellent fit to the data. Estimation of the contribution of higher p levels allows extraction of a value and sign for $R = +1.0012(12)$. This result is combined with recent measurements of the lifetime of the resonance transitions in Na to obtain a value for the ratio of excited-state transition-matrix elements for the $3p^2P_j \rightarrow 5s^2S_{1/2}$ transition ($j=3/2$ compared to $j=1/2$) of $1.0013(15)$. [S1050-2947(97)09001-X]

PACS number(s): 32.70.Cs, 32.70.Fw, 32.80.Wr, 33.80.Wz

INTRODUCTION

Development of new measurement techniques and refinement of older technologies has led to substantial improvement in determination of many atomic properties. Considering some examples for the Na atom, the recently developed atom interferometer has been applied to precise measurement of the polarizability of atomic sodium in the $3s^2S_{1/2}$ ground level [1]. In another area, a number of techniques have been applied to measurement of the lifetime of the resonance transitions in Na. Among these is direct measurement [2] of the natural width of the $3s^2S_{1/2} \rightarrow 3p^2P_{3/2}$ transition in a sample of very cold Na atoms for which the Doppler width was a small fraction of the total transition width. Diatomic molecular spectroscopy of very weakly bound Na_2 molecules in an atom trap has allowed the determination [3] of the so-called C_3 coefficient, from which the transition dipole strength of the $3s^2S_{1/2} \rightarrow 3p^2P_{1/2}$ transition may be extracted. Finally, the lifetime of both resonance transitions in Na has been recently determined to very high precision by using a refinement of beam-gas-laser spectroscopy [4]. Concentration on atomic sodium has been motivated by a long-standing discrepancy between experiment and theory for the two lightest alkali-metal atoms, Li and Na.

In this paper we report on an experimental approach that can yield precise determination of relative atomic or molecular transition matrix elements, including the sign. When corresponding absolute values are available for one of the quantities, then the other member of the ratio may be put on an absolute scale. This approach is particularly useful when one of the two matrix elements is much larger than the other, and thus may be more readily determined to good accuracy. Important information may also be extracted when the ratio of matrix elements itself has a particular limiting value in some approximation. Then departures from the limiting value indicate breakdown of the approximation.

The technique used here is two-photon, two-color polarization spectroscopy. In this approach, two separate light

sources are tuned so as to resonantly excite a dipole-allowed two-photon transition. Variations of the relative polarizations of the light sources generate a polarization ratio. When more than one intermediate level contributes significantly to the process, there is interference between the amplitudes from the levels. This interference can be revealed in a polarization ratio, and modeling of the experimental ratio allows determination of the size of the interference term relative to either of the individual transition-matrix elements. In atoms, interferences may be between fine or hyperfine levels, or between levels from different electronic configurations. Both fine and hyperfine interferences similar to those considered in the present paper have previously been observed in Rayleigh scattering in Na [5,6], and, under severe collisional conditions, in s - s and s - d two-photon transitions [7,8]. Fine-structure destructive interference has also been demonstrated by Bjorkholm and Liao [9], on the excitation spectrum of the $3s^2S_{1/2} \rightarrow 3p^2P_j \rightarrow 4d^2D_j$ transition of Na. Finally, we point out that, in diatomic molecular spectroscopy, interferences could additionally arise between rotational branches connecting selected initial and final levels. Exchange interferences between rotational branches associated with different vibrational transitions are also possible.

In the present report, we are concerned with the $3s^2S_{1/2} \rightarrow 5s^2S_{1/2}$ two-photon transition in atomic Na, for which the dominant intermediate levels are the components of the $3p^2P_j$ ($j=1/2, 3/2$) fine-structure doublet. There is strong interference between the transition amplitudes through the different fine-structure components. Because of the different angular momentum j of each component, this interference is revealed directly in a polarization spectrum obtained by varying the relative frequencies of the two light sources used, but in such a way that the two-photon resonance condition is always met. The spectral distribution of polarization contains information on the relative transition-matrix elements through the two components, and may be modeled so as to determine the ratio of matrix elements. For atoms with very weak spin-orbit interaction, a value of 2 is

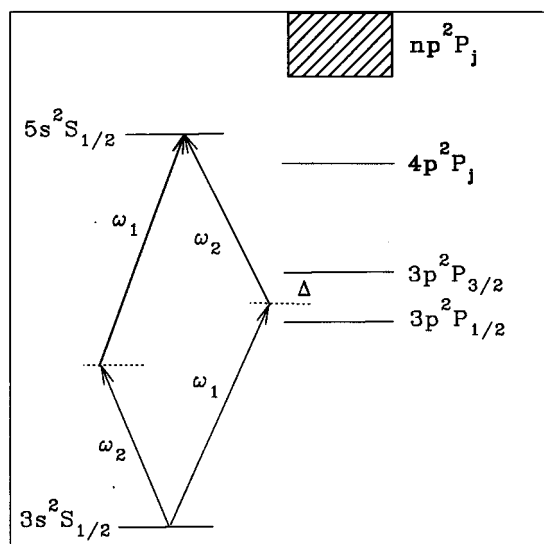


FIG. 1. Partial schematic energy level diagram for Na, illustrating the two-photon excitation scheme used in the experiment.

expected for the corresponding intensity ratio. But the spin-orbit potential is generally attractive for one fine-structure component and repulsive for the other. Thus, for heavy atoms with large spin-orbit interaction, departure from a ratio of 2 is generally anticipated on some level [10]. In fact, strong departures from this value have been measured in the $n s^2 S_{1/2} \rightarrow n' s^2 P_j$ of the heavier alkalis [10–13], with the largest effects being observed in Cs [14]. The anomaly extends beyond the ionization limit, where it is revealed as a minimum in the photoionization cross section [15–17]. In the following sections, the basic scheme of the experiment is described and details of the experimental procedure presented. These are followed by a presentation and discussion of our results. Combination of precise measurements of the ratio of transition elements for the resonance transitions from other sources [4] are then used to extract the ratio of excited-state transition-matrix elements for the $3 p^2 P_j \rightarrow 5 s^2 S_{1/2}$ transition ($j = 3/2$ compared to $j = 1/2$).

EXPERIMENTAL APPROACH

The basic experimental scheme is illustrated in Fig. 1, which shows a partial energy-level diagram for low-lying levels of atomic Na. There, the frequencies of two light sources, laser 1 with frequency ω_1 and laser 2 with frequency ω_2 , are adjusted so that $\omega_1 + \omega_2 = \omega_0$, where ω_0 is the frequency of the $3 s^2 S_{1/2} \rightarrow 5 s^2 S_{1/2}$ transition in atomic Na. The location of the virtual intermediate level is referenced to an atomic level by definition of a detuning $\Delta = \omega_1 - \omega_{3/2}$ of the laser 1 frequency from one-photon resonance. Monitoring of the two-photon resonance condition is accomplished by collection and detection of the fluorescence from the $4 p^2 P_j \rightarrow 3 s^2 S_{1/2}$ cascade transition at 330.2 nm. The main part of the signal in the experiments comes from the nearly resonant (for $\omega_1 + \omega_2$ ordering of absorption) $3 p^2 P_j$ levels. However, at the level of precision of the experiment, both the exchange order of absorption ($\omega_2 + \omega_1$) and more energetic p levels contribute significantly to the signals, and must be included in modeling the process.

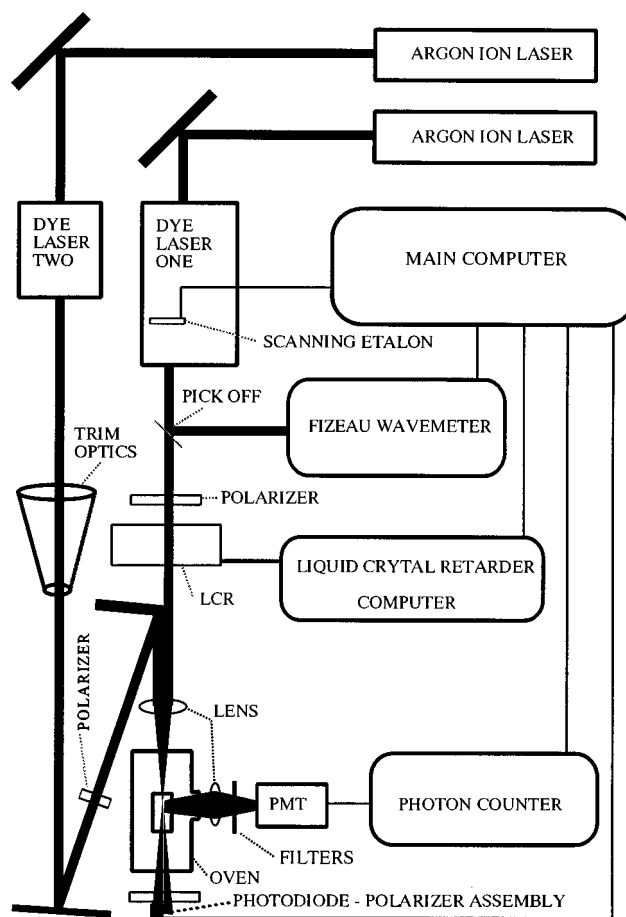


FIG. 2. Block diagram of the experimental apparatus.

A diagram of the basic experimental apparatus is shown in Fig. 2, where it is shown generally that the main experimental instrumentation, including the laser scanning, polarimeter, and signal acquisition and storage are all controlled by the main computer. As shown in the figure, the two dye lasers are each pumped by separate Ar^+ lasers. Laser 1 is a broadband ring dye laser operating around 590.0 nm, in the vicinity of the Na resonance transitions. It has a typical output power of 850 mW. The laser bandwidth of about 0.2 cm^{-1} is determined by an intracavity uncoated quartz etalon of 0.1 cm thickness. The etalon is mounted on a galvanometer, which permits smooth tilt tuning of the laser, without mode hops, over a range of about 1.0 cm^{-1} . A portion of the laser 1 output is directed into a Fizeau wave meter, which has a precision of 10^{-2} cm^{-1} , and which is calibrated absolutely against the well-known Na resonance frequencies and the HeNe laser line at 632.8 nm. The wave meter monitors quascontinuously the output frequency of laser 1, thus providing measurement of the detuning Δ of the laser from atomic resonance. The beam is then passed through polarizing optics consisting of a thin-film type linear polarizing filter and an electronically controlled liquid-crystal variable retarder (LCR). This machine allows for variation of the direction of linear polarization of laser 1 to be parallel or perpendicular to that of laser 2. The beam is then weakly focused with a 30-cm focal length lens into a heated oven containing a Pyrex sample cell filled with a small amount of Na metal. The cell windows were mounted normal to the

laser beam direction, in order to minimize variations in their transmission with polarization. The oven temperature was maintained at 473 K within ± 0.2 K by means of a temperature controller, which provided power for the oven heaters and for thermocouple-monitored temperature measurement and feedback. The Na atom vapor density in the Pyrex sample cell was $\sim 4 \times 10^{12}/\text{cm}^3$.

Laser 2 is a standing-wave dye laser having a maximum output power of 450 mW and an average bandwidth of 0.15 cm^{-1} determined also by a 0.1-cm-thick quartz etalon. It operates at a wavelength of about 616 nm, in the vicinity of the $3p^2P_j \rightarrow 5s^2S_{1/2}$ transition. The line shape for the laser 2 output is slightly asymmetric, but this has no measurable effect on the final results. A set of trimming optics is used to adjust the laser 2 beam spatial profile to match the size and divergence to that of laser 1. The laser 2 output beam is then passed through a Glan-Thompson linear polarizer, which is used to define the linear polarization direction relative to that of laser 1. The beam is focused into the oven-sample cell arrangement by the 30-cm focal length lens used to focus laser 1. The two beams have a diameter of approximately 3 mm, and are separated by this amount on the surface of the focusing lens. This results in a minimum beam waist of about 10^{-3} cm^{-1} and an intersection angle of around 10^{-2} rad in the viewing region of the cell.

The two-photon resonance signals are monitored by a photomultiplier tube–optical filter combination located at right angles to the direction of propagation of the laser beams. The filters, consisting of two type UG-11 glass absorption filters and a 10-nm bandpass interference filter, transmit about 25% of the fluorescence arising from the $4p^2P_j \rightarrow 3s^2S_{1/2}$ cascade transition around 330.2 nm. Since excitation of the $5s^2S_{1/2}$ level is accomplished with linearly polarized light, and done without hyperfine selectivity or applied magnetic field, the fluorescence signals used for monitoring the excitation are a direct measure of the population generated in the $5s^2S_{1/2}$ level. Note that this is not the case if an orientation is generated in the excited level, or if there is partial or total resolution of the excited-level hyperfine structure [18]. A 4-cm focal length lens is used to gather the fluorescence light, resulting in counting rates in the range 10^3 – 10^5 s^{-1} , depending on Δ . Background rate due to dark current was typically 10 s^{-1} , while laser 1 and laser 2 generated low-level backgrounds of about 10 and 5 s^{-1} , respectively. These rates, which were independent of the polarization state of either laser, were subtracted from the measured rate to get the true counting rates used in the analysis. Signals from the photomultiplier tube were collected in a 300-MHz photon counter, which provided for lower and upper level discrimination, and for pulse amplification, shaping, and counting. This unit communicated with the main control computer via a RS232 serial communication port.

The normal experimental procedure was to fix the laser 2 frequency at some value, corresponding to a desired nominal detuning of laser 1. Then laser 1 was tuned over the two-photon resonance, with the scan partitioned into 200 steps for the approximately 1-cm^{-1} scan. At each step of the scan, the polarization state of laser 1 was alternated once per second to be either parallel or perpendicular to that of laser 2, and the signal recorded in each case. The procedure minimized systematic small drifts in the relative intensities due to

fluctuations in laser power, atom density, and alignment. In addition, because of the approximately 40-ms response time of the liquid crystal retarder, a 400-ms delay was inserted between the each change of polarization state and the resumption of data acquisition. Each scan was several minutes long, depending on counting rate. The scan interval was adjusted so as to maintain approximately constant photon counting statistics in each detection channel, independent of detuning Δ . After correction for background levels, the main quantities of the experiment are formed by summation of the signals in the parallel and perpendicular polarization channels. These summed, and corrected, signals are labeled as I_{\parallel} and I_{\perp} . From them, a linear polarization degree P_L is formed. This quantity is defined as

$$P_L = \frac{I_{\parallel} - I_{\perp}}{I_{\parallel} + I_{\perp}}. \quad (1)$$

In order to minimize systematic errors in experimental determination of P_L , special care was taken to produce both a very high level of linear polarization along a common axis for each laser beam in the interaction region of the cell, and to ensure stable and high-quality rotation of the linear polarization direction of laser 1 by $\pi/2$ relative to the common axis. Two general tests are used to assess the quality of the polarimeter, these being an extinction ratio test and a 45° test. To accomplish these assessments, a Glan-Thompson, and a Wollaston prism polarizer are used; each of these devices has a quoted extinction ratio of 1:10 000. As shown in Fig. 2, the Glan-Thompson prism is located in laser beam 2, while the Wollaston prism is situated after the sample cell and oven location. In the extinction test, the transmission of the laser beams by the Wollaston prism, which splits an incoming beam into two separate beams of orthogonal linear polarization, is used to determine the relative intensities of the laser beams in different polarization states. First, the Glan-Thompson prism in laser beam 2 is adjusted for maximum transmission of the beam. Then the Wollaston prism is oriented properly for minimum transmission in one of its channels and maximum in the other. This defines one of the two orthogonal axes necessary for the polarization measurements. The normal polarization state of beam 1 is perpendicular to that of beam 2, and so the minimum transmission channel for laser beam 1 is the maximum channel for beam 2, and vice versa. The photographic quality polarizer in laser beam 1 may be adjusted slightly so that this is the case. With proper voltage applied to the liquid-crystal polarization rotator in the laser beam 1 path, the linear polarization is rotated by $\pi/2$. This is the so-called parallel state; in this case the minimum transmission channels for the Wollaston prism are the same for both beams. With fine adjustments of the retardance of the LCR, extinction ratios of 1:8000 could be achieved with the polarimeter.

A second type of test is necessary to ensure proper measurements of linear polarization degree. In the present experiment we use a 45° test to ensure that the relative intensities and physical overlap of the two laser beams are maintained during the polarization switching process. Such changes could arise from differential Fresnel reflection from the cell windows, slight changes in the transmission of the LCR for the two different polarization states, or from

changes in the beam shape or direction of propagation for the parallel and perpendicular states of polarization. In this test, the experimental fluorescence signal itself is used as a monitor, so that changes in the measured intensities could be directly determined. To accomplish the measurements, the Glan-Thompson polarizer is rotated by $\pm 45^\circ$ from its normal orientation. Then the switching of the polarization state of laser 1 produces no change in the physical geometry of the two-photon excitation, and the measured linear polarization must be zero. This null test of the channel balance is limited chiefly by counting statistics, and so is most profitably done nearer the resonance transitions. However, in the region where the measured P_L is normally zero, the test is meaningless. Thus this test was mainly done in the spectral region near the $D2$ transition. The resulting polarimeter had an analyzing power better than 1:3000. Finally, a photodiode was used with the Wollaston prism during normal data acquisition in order to monitor proper polarization switching.

RESULTS AND ANALYSIS

The main results of the experiment are measurements of the linear polarization degree P_L as a function of detuning Δ . For very narrow band laser beams, the linear polarization degree is formed from the following intensity expressions, obtained in a weak field, rotating wave approximation, for the two polarization configurations [19]:

$$I_{\parallel} = I_0 \left[\frac{2R}{\omega_1 - \omega_{3/2}} + \frac{1}{\omega_1 - \omega_{1/2}} + \frac{2R}{\omega_2 - \omega_{3/2}} + \frac{1}{\omega_2 - \omega_{1/2}} + P \right]^2, \quad (2)$$

$$I_{\perp} = I_0 \left[\frac{R}{\omega_1 - \omega_{3/2}} - \frac{1}{\omega_1 - \omega_{1/2}} - \frac{R}{\omega_2 - \omega_{3/2}} + \frac{1}{\omega_2 - \omega_{1/2}} + Q \right]^2.$$

In the expressions, I_0 is an overall normalizing constant proportional to the product of intensities of the two laser beams, R is a ratio of transition matrix elements [20], while P and Q represent the contribution of all higher energy levels. The frequencies of the two laser beams are ω_1 and ω_2 , while $\omega_{3/2}$ and $\omega_{1/2}$ are the frequencies of the $3s^2S_{1/2} \rightarrow 3p^2P_{3/2}$ and $3s^2S_{1/2} \rightarrow 3p^2P_{1/2}$ transitions. For exact two-photon resonance, the sum $\omega_1 + \omega_2 = \omega_0$, where ω_0 is the $3s^2S_{1/2} \rightarrow 5s^2S_{1/2}$ energy separation. These values [21] are given by $\omega_{3/2} = 16\,973.37(1) \text{ cm}^{-1}$, $\omega_{1/2} = 16\,956.17(1) \text{ cm}^{-1}$, and $\omega_0 = 33\,200.69(1) \text{ cm}^{-1}$. In fitting and modeling the polarization spectra, the expressions for the intensity are given as a function of detuning Δ , as defined in the previous section:

$$I_{\parallel} = I_0 \left[\frac{2R}{\Delta} + \frac{1}{\Delta + \Delta_{fs}} + \frac{2R}{\omega_0 - 2\omega_{3/2} - \Delta} + \frac{1}{\omega_0 - 2\omega_{3/2} + \Delta_{fs} - \Delta} + P \right]^2, \quad (3)$$

$$I_{\perp} = I_0 \left[\frac{R}{\Delta} - \frac{1}{\Delta + \Delta_{fs}} - \frac{R}{\omega_0 - 2\omega_{3/2} - \Delta} + \frac{1}{\omega_0 - 2\omega_{3/2} + \Delta_{fs} - \Delta} + Q \right]^2.$$

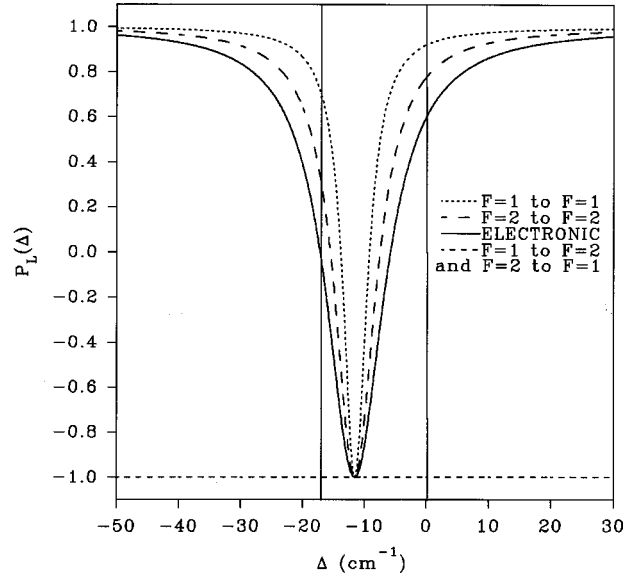


FIG. 3. Electronic and hyperfine linear polarization spectra in the vicinity of the Na resonance lines.

In the second and fourth terms of Eq. (3), where the fine-structure splitting appears directly, an additional digit of accuracy is used from the extremely well-known fine-structure splitting [22] in the $3p$ level in Na, $17.195\,910(60) \text{ cm}^{-1}$.

The quantity R is defined as a j -dependent ratio of reduced matrix elements,

$$R = \frac{\langle 5s \| r \| 3p(j=3/2) \rangle \langle 3p(j=3/2) \| r \| 3s \rangle}{\langle 5s \| r \| 3p(j=1/2) \rangle \langle 3p(j=1/2) \| r \| 3s \rangle} \quad (4)$$

for the $3p$ multiplet. In the absence of spin orbit, or other relativistic perturbation, R normally equals 1. In this definition of R , a factor of 2 has been removed in order to obtain an $R=1$ nonrelativistic limit. This factor is explicitly included in Eq. (3), which yields the proper nonrelativistic intensity ratio of 2 for resonance excitation of the multiplet components, calculated as the ratio of the total intensity ($I_{\parallel} + 2I_{\perp}$). Of course, then the singularity must be removed by inclusion in Eq. (3) the natural width of the transitions. In the heavier alkali atoms, which have quite large spin-orbit interactions, R varies significantly from unity. The quantity P , which represents the contribution of all more energetic levels is given, to an excellent approximation, by

$$P = \sum_{n>3} \left[p_n \left(\frac{3}{\omega_1 - \omega_n} + \frac{3}{\omega_2 - \omega_n} \right) \right], \quad (5)$$

where

$$p_n = \frac{\langle 5s \| r \| np \rangle \langle np \| r \| 3s \rangle}{\langle 5s \| r \| 3p(j=1/2) \rangle \langle 3p(j=1/2) \| r \| 3s \rangle}. \quad (6)$$

In Eq. (5), the fine-structure splitting of the $n>3$ p multiplets has a negligible effect on the value of P , and so it has been ignored. This is an excellent approximation because relativistic contributions to P are suppressed by a *difference* in frequency-dependent terms, rather than the *sum* as in Eq. (5). At this level of approximation, $Q=0$. Physically, this

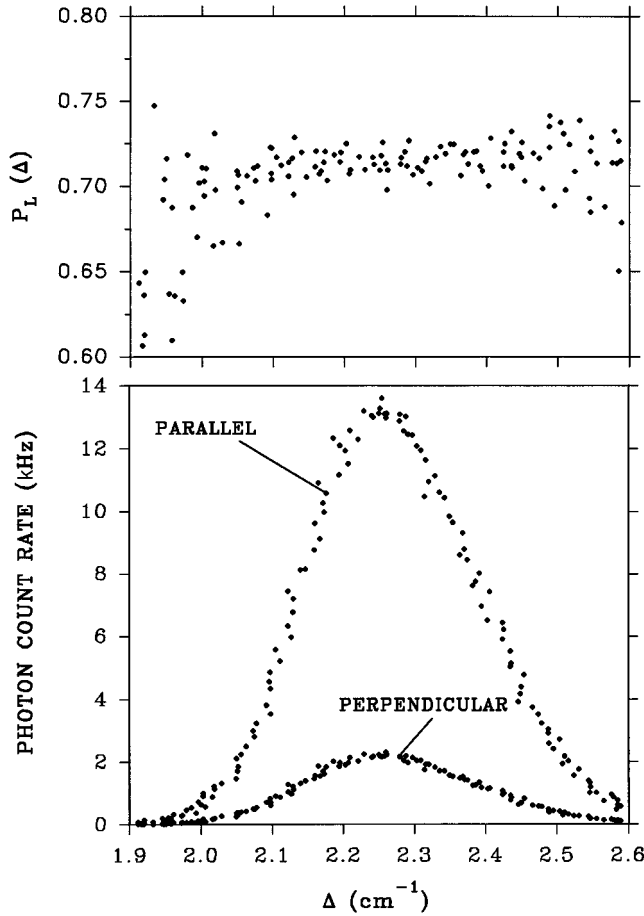


FIG. 4. Typical two-photon excitation line shape and associated variation of linear polarization.

corresponds to coherently exciting the $n p^2 P_j$ multiplet states as if they were degenerate, and with j -independent weight from the radial integrals. Then the spin plays no role in determining the polarization, and $P_L = 100\%$. The general features of P_L resulting from Eq. (3), for the case $R=1$, $P=0$ are shown in Fig. 3. There it is seen that the polarization ranges from $+100\%$ at larger detunings to -100% at a critical detuning of $\Delta_c = -2\Delta_{fs}/3$, where $I_{||}=0$. The resonance line values of 60% for the $D2$ transition and 0% for the $D1$ transition are what are expected in the absence of hyperfine depolarization of the resonance radiation [23]. Generally, the shape of the spectrum and the location of Δ_c depend on the values of R and P .

The above expressions neglect the hyperfine structure in the $3 s^2 S_{1/2}$ and $5 s^2 S_{1/2}$ levels [24]. In the present experiment, this is justified because the P_L spectrum is measured with broadband lasers scanned over the two-photon resonance. Then the spectrum is independent of the underlying hyperfine-dependent variations in polarization. Note that these variations are not small; our calculation of the variations is presented as the various chain curves in Fig. 3. Because of the particularly rapid variations between the D lines of the $\Delta F=0$ transitions, care must be taken that the spectral averaging over hyperfine components is complete. For this purpose, the spectra were measured with copropagating laser beams, when the Doppler width is approximately double that for a single photon transition.

TABLE I. Contributions of various systematic effects to the total error in the measured polarization.

Quantity	Uncertainty
Detuning, Δ	$\pm 0.02 \text{ cm}^{-1}$
Analyzing power (maximum)	0.033%
Laser power (maximum)	0.030%
Vapor density	0.02%
Linearity	0.0001%
Statistics	0.20%
Total	0.21%

Systematic tests and estimated errors

As described earlier, the normal experimental procedure consisted of fixing the frequency of laser 2, and scanning laser 1 over the two-photon resonance. The result of a typical scan is presented in Fig. 4, which is taken at a nominal detuning of $\Delta \sim +2.3 \text{ cm}^{-1}$. In the figure, the lower portion shows the detuning-dependent intensity in the two polarization channels, while the upper portion gives the corresponding linear polarization degree as a function of the nominal laser 1 detuning from $D2$ resonance. The slight asymmetry in the spectral profile of laser 2 indicated in the previous section is evident in the line shape for the process. The spectral width at half-maximum of about 0.25 cm^{-1} (7.5 GHz) is a convolution of the laser linewidths, the summed Doppler width of approximately 3 GHz, and the ground-state Na hyperfine splitting of 1.77 GHz. The polarization given in the upper panel shows a slight increase with increasing detuning of laser 1. This is due to the overall shape of the electronic polarization spectrum, as shown in Fig. 3.

The main sources of systematic effects considered in the experiment are possible variations of the measured P_L with Na density, the power of laser 1 or laser 2, and background. The reliability of the wave meter to produce accurate detun-

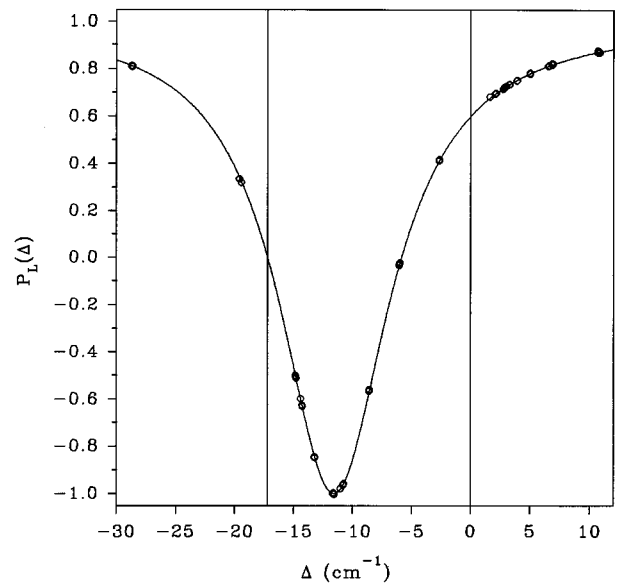


FIG. 5. Measured linear polarization spectrum in the vicinity of the Na resonance lines.

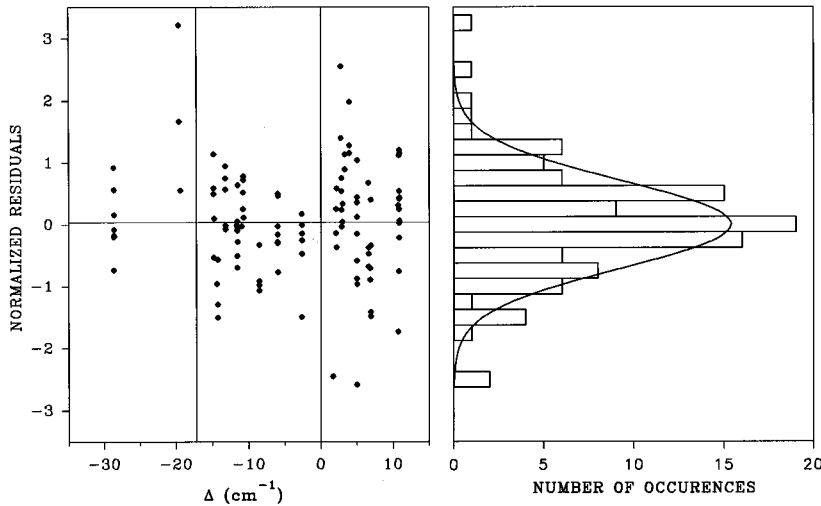


FIG. 6. Distribution of normalized residuals of the fit to the polarization spectrum of Fig. 5.

ings was also assessed. The limits of reliability of the polarimeter as an instrument are discussed in the previous section. Tests to evaluate effects of Na density and laser power were conducted at relatively small detunings of about 2 cm^{-1} , where the signal size is large, and where possible light shifts [25,26] associated with either laser would be largest. Variations in Na density over a factor of about 50 produced no discernible systematic variation of the measured polarization, and provided an upper limit of about 0.02% variation in P_L over this range. Similarly, variations in the power of laser 1 or laser 2 (with the other held fixed) over a factor of 10 revealed no systematic variations, and set upper limits for variations of 0.025% for laser 1 and 0.02% for laser 2. Background levels due to leakage of laser light through the filters in the detections channel and due to dark current were assessed for each experimental data run, and were subtracted from the raw counting rates before forming the polarization ratio. As is evident from Fig. 4, the background was small in comparison to the signal sizes, with peak counting rates being on the order of 10^4 s^{-1} and total background and dark levels being around 20 s^{-1} . No patterns of variations in background with detuning were observed. Statistical background fluctuations thus had very little effect ($\sim \pm 0.03\%$) on the total uncertainty. This is included in the quoted statistical fluctuations in P_L . Estimates of the systematic uncertainty in P_L due to these quantities, along with typical uncertainty due to counting statistics alone, are summarized in Table I.

Experimental results and analysis

The measured polarization spectrum is presented in Fig. 5. In the figure, the error bars on the detunings ($\sim 0.02 \text{ cm}^{-1}$) and on P_L (typically 0.2%) are too small to display. Note that some of the data points are strongly blended with others at very nearly the same detuning. The solid curve in Fig. 5 represents a weighted least-squares fit to the data points, with the quantities R and P as fitting parameters. In the fitting, the quantity P , which depends very weakly on Δ through the frequency-dependent denominator, is treated as a constant. The measurements at each detuning are compared to $P_L(\Delta)$ given by Eq. (1) and Eq. (3), with intensity expressions averaged over a convolution of the Doppler width and the measured line shape of each laser, and accounting for variations

with detunings of both I_0 and the displayed frequency-dependent part of Eq. (3). Residuals to the fit, normalized to the statistical error in each point, are presented in Fig. 6, where it is seen that they have a mean value consistent with zero, no evident spectral variations, and a distribution consistent with a statistical one.

The χ^2 minimum obtained in the fit, $\chi^2=84.12$ for the 109 data points is obtained *not* for unique values for R and P . Instead, as shown in Fig. 7, these quantities are found to be highly correlated, with a virtually constant minimum being found for the locus of values given by $R = 1.00243 + 5.673P$. Thus to obtain a unique value for R requires estimation of the contributions to the spectrum for p levels lying higher in energy than the $3p$ levels. To accomplish this, the quantities p_n [Eq. (5)] were gathered from several sources [27–30], assessed for consistency, and a set chosen for estimation of P . The magnitudes of the relative matrix elements are generally consistent at a better than 20% level. However, because the sign information is available, we have chosen the results of Bates and Damgaard [30], for the purpose of esti-

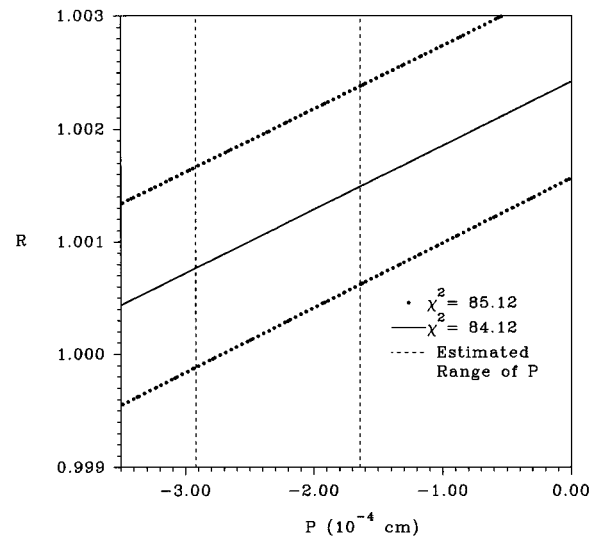


FIG. 7. Illustration of the correlation of the fitting parameters R and P , along with the boundary of the 1σ region. The vertical lines represent the estimated uncertainty in the calculated value of P .

inating P . This is possible in spite of the limited range of their results because the P sum is dominated by terms up to $n=6$. We obtain $P = -2.3(6) \times 10^{-4}$, where the 25% error is estimated from the range of variations in the relative magnitudes from the different sources. Although undoubtedly a more accurate value for the summation could be calculated, this estimate of itself yields a value for $R = 1.0012(12)$, with the error corresponding to the maximum range of $\chi^2 + 1$ values consistent with the quoted uncertainty in P .

According to Eq. (4), the quantity $R = R_2 R_1$ is a product of ratios of matrix elements connecting the ground, intermediate, and final levels involved in the transition. A number of recent precise and mutually consistent measurements of the lifetime of the Na resonance transitions permit evaluation of one of the individual ratios. Thus the ratio of *excited-state* matrix elements R_2 may be extracted to a precision similar to that of either measurement. Of the most recent measurements, Volz *et al.* [4] have measured the lifetime of both transitions. Thus we use their measurements to extract the ratio $R_1 = 0.9999(10)$. This yields the excited-state ratio of matrix elements for the $3p^2P_j \rightarrow 5s^2S_{1/2}$ transition of $R_2 = 1.0013(15)$. To our knowledge, this is the most precise measurement of a ratio of excited-state matrix elements (or equivalent oscillator strengths).

The present measurements show that relativistic perturbation of the transition-matrix elements in Na is very small. Such perturbation arises because the sign of the spin-orbit potential is different for the two different multiplet components, and thus the radial matrix elements are generally j dependent. Manifestation of the effect is not limited to transitions out of the ground level, although to our knowledge, observation has not previously been made of this effect for excited-state transitions. Thus the relative transition-matrix elements for the second step of the two-step transition could well exhibit a j dependence different from the first step. The variation of the relative reduced multiplet transition oscillator strengths for transitions out of the ground level is much larger in Rb and Cs than in Na. Experiments to measure this effect on excited-state transitions are currently under way in Rb.

It is important to note that the present technique also determines the relative *sign* of the ratio of matrix elements defined in Eq. (3). For example, if $R = +1$ and $P = 0$, the $P_L = -100\%$ point (see Fig. 3) is located at a detuning $\Delta_c = -2\Delta_{fs}/3$, while if $R = -1$, it is located outside the mul-

tiplet components at $\Delta_c = -2\Delta_{fs}$. Thus, in the present experiment, the results show that the ratio is positive. Further, although it is possible that the relative multiplet matrix elements have different signs, it is unlikely in the present case, because the oscillator strengths for the transitions are large and nearly equal. For there to be a sign change across the multiplet would imply that the matrix elements would go through a zero as a function of effective principal quantum number for both multiplet transitions. We thus conclude that the individual multiplet matrix elements have the same sign, and that R_1 and R_2 are separately positive.

SUMMARY

Precise measurements of a linear polarization spectrum of the $3s^2S_{1/2} \rightarrow 3p^2P_j \rightarrow 5s^2S_{1/2}$ transition in atomic Na have been made. The spectrum depends parametrically on ratios of reduced dipole matrix elements for the transition. These matrix elements are taken to be j dependent for the resonance transition, and the effect of more energetic p levels is taken into account. Extraordinary agreement between theoretical modeling of the process and the experimental results is obtained through a parametric relationship between the j -dependent ratio of reduced matrix elements R and a quantity P representing the contribution of other p levels. Combination of this result with recent precise measurements on the lifetime of the Na-resonance transitions, along with an estimate of P , has allowed precise determination of the relative dipole matrix elements for the excited-state $3p^2P_j \rightarrow 5s^2S_{1/2}$ transition. The method used may readily be applied to other transitions in atoms or in molecules, to obtain relative reduced transition-matrix elements to an approximately 10^{-3} level. Since the technique employed depends on interference among the transition elements, the relative sign of the amplitudes, and thus the matrix elements, may be determined. Finally, since the approach is essentially a spectroscopic one, it may be considered to be a mapping of matrix elements into the frequency domain, where they may be determined to high precision.

ACKNOWLEDGMENT

The financial support of the National Science Foundation under Grant No. NSF-PHY-9504864 is greatly appreciated.

-
- [1] C. R. Ekstrom, J. Schmiednayer, M. S. Chapman, T. Hammond, and D. E. Pritchard, *Phys. Rev. A* **51**, 3883 (1995).
 - [2] C. W. Oates, K. R. Vogel, and J. L. Hall, *Phys. Rev. Lett.* **76**, 2866 (1996).
 - [3] E. Tiemann, H. Richling, and H. Knöckel (unpublished).
 - [4] U. Volz, M. Jagerus, H. Liebel, A. Schmitt, and H. Schmoranz, *Phys. Rev. Lett.* **76**, 2862 (1996).
 - [5] A. C. Tam and C. K. Au, *Opt. Commun.* **19**, 265 (1976).
 - [6] R. Walkup, A. L. Migdall, and D. E. Pritchard, *Phys. Rev. A* **25**, 3114 (1982).
 - [7] D. Zei, R. N. Compton, J. Stockdale, and M. Pindzola, *Phys. Rev. A* **40**, 5044 (1989).
 - [8] L. Cook, D. Olsgaard, M. Havey, and A. Sieradzan, *Phys. Rev. A* **47**, 340 (1993).
 - [9] J. E. Bjorkholm and P. F. Liao, *Phys. Rev. Lett.* **33**, 128 (1974).
 - [10] Jon C. Weisheit, *Phys. Rev. A* **5**, 1621 (1972).
 - [11] Chou-Mou Huang and Charles C. Wang, *Phys. Rev. Lett.* **46**, 1195 (1981).
 - [12] E. Caliebe and K. Niemax, *J. Phys. B* **12**, L45 (1979).
 - [13] L. N. Shabanova and A. N. Khlyustalov, *Opt. Spectrosc.* **56**, 128 (1984).
 - [14] T. F. Gallagher, *Rydberg Atoms* (Cambridge University Press, Cambridge, 1996).

- [15] U. Fano and J. W. Cooper, *Rev. Mod. Phys.* **40**, 441 (1968).
- [16] U. Fano, *Phys. Rev.* **178**, 131 (1969).
- [17] W. Sandner, T. F. Gallagher, K. A. Safinya, and F. Gounand, *Phys. Rev. A* **23**, R2732 (1981).
- [18] C. H. Greene and R. N. Zare, *Annu. Rev. Phys. Chem.* **33**, 119 (1982).
- [19] R. Louden, *Quantum Theory of Light*, 2nd ed. (Oxford University Press, Oxford, 1992).
- [20] M. E. Rose, *Elementary Theory of Angular Momentum* (Wiley, New York, 1957).
- [21] C. E. Moore, *Atomic Energy Levels*, NSRDS-NBS Circular No. 35 (U.S. Department of Commerce, Washington, D.C., 1971), Vol. 1.
- [22] P. Juncar, J. Pinard, J. Hamon, and A. Chartier, *Metrologia* **17**, 77 (1981).
- [23] M. D. Havey and L. L. Vahala, *J. Chem. Phys.* **86**, 1648 (1987).
- [24] E. Arimondo, M. Inguscio, and P. Violino, *Rev. Mod. Phys.* **49**, 31 (1977).
- [25] P. F. Liao and J. E. Bjorkholm, *Phys. Rev. Lett.* **34**, 1 (1975).
- [26] Claude Cohen-Tannoudji, Jacques Dupont-Rec, and Gilbert Grynberg, *Atom-Photon Processes: Basic Processes and Interactions* (Wiley, New York, 1992).
- [27] W. L. Weise, M. W. Smith, and B. M. Miles, *Atomic Transition Probabilities: Sodium Through Calcium*, Natl. Bur. Stand. (U.S.) (U.S. GPO, Washington, D.C. 1966, 1969), Vols. 1, 2.
- [28] V. A. Kostelecky and M. M. Nieto, *Phys. Rev. A* **32**, 3243 (1985).
- [29] A. Lindgård and S. E. Hielson, *Atomic Data and Nuclear Data Tables* (Academic, New York, 1977), Vol. 19.
- [30] D. R. Bates and A. Damgaard, *Philos. Trans. R. Soc. London* **242**, 101 (1949).